Eur. Phys. J. A **7**, 355–360 (2000)

THE EUROPEAN PHYSICAL JOURNAL A

Isospin effects on the GDR in Vlasov Method

J.S. Wang[2,a], W.Q. Shen[1,2], Y.H. Cai[1,2,4], Y.G. Ma[1,2,3], J. Feng[1,2], D.Q. Fang[2], X.Z. Cai[2], Q.M. Su[2]

[1] CCAST (World Laboratory), P.O. Box 8730, Beijing 100080, P.R. China
[2] Institute of Nuclear Research, Chinese Academy of Sciences, Shanghai 201800, P.R. China
[3] Fudan-T.D.Lee Physics Laboratory, Fudan University, Shanghai, 200433, P.R. China
[4] Center of Theoretical Nuclear Physics, National Laboratory of Heavy Ion Accelerator, Lanzhou, 730000, P.R. China

Received: 20 February 1999 / Revised version: 21 May 1999
Communicated by P. Schuck

Abstract. The systematics of the isovector Giant Dipole Resonance (GDR) is studied via the microscopic semi-classical Vlasov method. The calculated results of the peak energy and the widths (FWHM) of the GDR strength distribution can reproduce the experimental data and follow the empirical formula. The isospin effects on the peak energy and the widths of the GDR strength distribution are found small and these effects increase slightly with the $(N-Z)/A$. The characteristics of the GDR have been studied as a function of the temperature in very heavy compound systems ($A > 300$). The interplay between one-body damping and two-body damping is also discussed.

PACS. 24.30.Cz Giant resonance – 20.60.Ev collective model

1 Introduction

GDR built on excited states of hot nuclei has been intensively researched both experimentally and theoretically in the recent decades [1–3]. Some properties of the GDR have been well established. The spectrum of the GDR γ rays has a good Lorentzian shape. Moreover, this spectrum strongly depends on the other nuclear degrees of freedom, such as nuclear shape and angular momentum. So, the GDR γ rays is a good probe to provide us more informations on properties of hot nuclei: the shapes and fluctuation of hot nuclei, fission delay and dissipative effects in hot-fission-unstable nuclei etc..

With the availability of newly constructed radioactive beam lines and 4π detector systems now and in the future, it becomes possible to study the properties and decay of the hot nuclei far from β stability line. So, it is important to know whether the theory describing the GDR for nuclei around the β stability line can be extrapolated to drip-line regions and what the characteristics of the GDR will be in such region. The quantum random phase approximation (RPA) is quite successful in describing the collective mode of the nucleus. It can give the main characteristics of many closed shell nuclei although it is complicated to work and not very transparent in results. Recently, people apply this method to nuclei far from the β stability line, or with high spin and super-deformed shape etc.. Z.Y. Ma et al. [4–5] and N.V. Giai et al. [6] studied the changes of the GDR for different Ar isotopes using RPA based on the Relativistic Mean Field theory (RRPA). I. Hamamoto et al. [7–8] have combined the RPA with self-consistent Hartree-Fork theory to study the characteristics of the GDR for the nuclei around the drip-line. In our paper, GDR are studied systematically in the frame of the semi-classical microscopic Vlasov method and the experimental systematics of the peak energy of GDR strength distribution can be well reproduced. Then we extend this framework to investigate the isospin effects on the isovector GDR by introducing the Woods-Saxon potential with different parameters for neutron and proton respectively.

It is a very interesting subject to study the formation and properties of super-heavy nuclei. Many research works [9–10] show that fission delay is in the order of 10–20 s for the compound nuclei formed in heavy ion reactions with the temperature at about $1 \sim 2$ MeV. One may expect, therefore, if the fission delay still exists in very heavy nucleus collisions, the Super Heavy Compound System (SHCS) would exist within a time long enough to build the GDR and decay by γ rays emission before fission. Such GDR γ rays then can be considered as a direct evidence of the formation of the SHCS. There have already been two experiments performed to study the formation of the SHCS via the possible GDR γ rays emission [11–12]. The data is still under analysis. However, there is still no theoretical research on such heavy compound system for the GDR γ rays emission. In this article, the characteristics of the GDR have been studied in such heavy compound systems (supposing it is ever formed in heavy ion reactions).

[a] *Present address:* Institute of Modern Physics, Chinese Academy of Sciences, 253 Nanchang Rd., 730000 Lanzhou, P.R. China

2 The Model

The microscopic semi-classical Vlasov method is developed from Vlasov equation, a semi-classical limit of the time dependent Hartree-Fork (TDHF) theory, to calculate the collective excitation in the nucleus. This method is similar to the Random-Phase-Approximation (RPA) which is a successful but complicated method in the nuclear physics. In the microscopic Vlasov method, temperature is considered straightforward with the $T \neq 0$ Fermi distribution of the energy level. It is convenient to study the interplay between the one-body and two-body damping by introducing the collision term in the Vlasov equation with the relaxation time method. The detail description of the microscopic Vlasov method can be found in [13–15]. The Vlasov equation with collision term can be described as the following,

$$\frac{\partial f}{\partial t} = \{h + \beta Q, f\} - \frac{f - f_0^*}{\tau_R}, \tag{1}$$

where, f is the single particle probability density, f_0^* is the new equilibrated density, τ_R is the relaxation time. βQ is an external driving term, h is the self-consistent single particle hamiltonian,

$$h(\vec{r}, \vec{p}, t) = \frac{\vec{p}^2}{2m} + U(\vec{r}, t), \tag{2}$$

The temperature dependent relaxation time $\tau(T)$ is chosen as a function of excitation energy ("temperature"):

$$\frac{\hbar}{\tau(T)} = \frac{\hbar}{\tau_0} + \frac{\hbar}{\Delta\tau(T)}, \tag{3}$$

where, $\frac{\hbar}{\tau_0}$ is zero temperature contribution, it is the sum of volume part $\left(\frac{\hbar}{\tau_0}\big|_{Vol}\right)$ and surface part $\left(\frac{\hbar}{\tau_0}\big|_{Surf}\right)$. Details can be found in [15–16]. $\frac{\hbar}{\Delta\tau(T)}$ is non-zero temperature contribution with $\Delta\tau(T) = 3.45T^{-2} + 0.392T^{-1/2}$, a modified expression of [17].

By introducing the response function, the response strength of the Giant Resonance without residual interaction is derived as the following (L denotes the multipolarity),

$$S_L^0(\omega) = -\frac{1}{\pi}\beta_L^0(\omega) \tag{4}$$

$\beta_L^0(\omega)$ is the imaginary party of the free polarization propagator,

$$\begin{aligned} \Pi_L^0(\omega) &= \alpha_L^0 + i\beta_L^0 \\ &= \frac{\pi}{2L+1}\sum_{n,N}\int dE F'(E)\int \lambda d\lambda \left|Y_{LN}\left(\frac{1}{2}\pi, \frac{1}{2}\pi\right)\right|^2 \\ &\quad \times T\frac{\tilde{\omega}_n(N)}{\omega - \tilde{\omega}_n(N)}|\tilde{Q}(n,N)|^2\big|_{E=E_f}, \end{aligned} \tag{5}$$

with poles at,

$$\tilde{\omega}_n(N) = n\frac{2\pi}{T} + N\frac{\Gamma}{T} - \frac{i}{\tau_R} = \omega_n(N) - \frac{i}{\tau_R}, \tag{6}$$

where, Γ is angular "period" and T is period of the radial motion. $\tilde{Q}(n,N)$ is complex residues,

$$\tilde{Q}(n,N) = A + Bi, \tag{7}$$

with

$$A = \frac{2}{T}\int_{r_1}^{r_2} dr \frac{Q_L(r)}{V(r)}\cos[S_n(N,r)]\cosh\left[\frac{\tau(r)}{\tau_R}\right], \tag{8}$$

$$B = \frac{2}{T}\int_{r_1}^{r_2} dr \frac{Q_L(r)}{V(r)}\sin[S_n(N,r)]\sinh\left[\frac{\tau(r)}{\tau_R}\right], \tag{9}$$

Contributions come from single particle orbits, in the mean field, with the angular momentum λ and the energy around the Fermi energy. Everything can be expressed in terms of radial and angular properties of these orbits, for a given multipole field $Q_L(r)$, r_1 and r_2 are classical turning points, $V(r)$ is radial velocity field. The phase $S_n(N,r)$ is,

$$S_n(N,r) = \omega_n(N)\tau(r) - N\psi(r) \tag{10}$$

where, $\tau(r)$ is time elapsed and angle spanned to reach the point r on the orbit (λ, E), N and n are integers, $-\infty < n < \infty$ and $-L \leq N \leq L$ respectively, with $(-1)^N = (-1)^L$. Details can be found in [13–15]

The equilibrated single particle probability density is taken in the form of a general Fermi distribution for the excited state with temperature T,

$$f_0 = F(E) = \frac{2}{(2\pi\hbar)}\frac{1}{1 + \exp\left(\frac{E - E_f}{T}\right)}, \tag{11}$$

The giant resonance strength formalism with the residual interaction is then as the following :

$$\begin{aligned} S_L(\omega) &= -\frac{1}{\pi}\,\mathrm{Im}\Pi_L(\omega) \\ &= \frac{S_L^0(\omega)}{(1 - \kappa(L)\alpha_L^0(\omega))^2 + \kappa(L)^2\pi^2 S_L^{0^2}(\omega)} \end{aligned} \tag{12}$$

where, $\kappa(L)$ is the coupling constant of the separable force (multipole-multipole type).

In the calculations we use the Woods-Saxon potential for the proton and neutron separately,

$$\begin{cases} U_q(r) = \dfrac{U_{0q}}{1 + \exp[(r-R)/a]} + \dfrac{\lambda_q^2}{2mr^2} + V_c & q = p \\ U_q(r) = \dfrac{U_{0q}}{1 + \exp[(r-R)/a]} + \dfrac{\lambda_q^2}{2mr^2} & q = n \end{cases} \tag{13}$$

Where, the first term is Woods-Saxon potential, the interaction radii $r = 1.30 \times A^{1/3}$ fm, $a = 0.65$, $U_{0p} = -75$ MeV, U_{0n} is chosen in order to have the correct number of protons and neutrons with the same Fermi energy $E_f^p = E_f^n$. The second term is centrifugal potential due to the angular momentum, V_c is the coulomb potential of a homogeneously charged sphere for protons. The coupling constant $\kappa_p(L)$ (for proton) and $\kappa_n(L)$ (for neutron) are taken as in [15, 18].

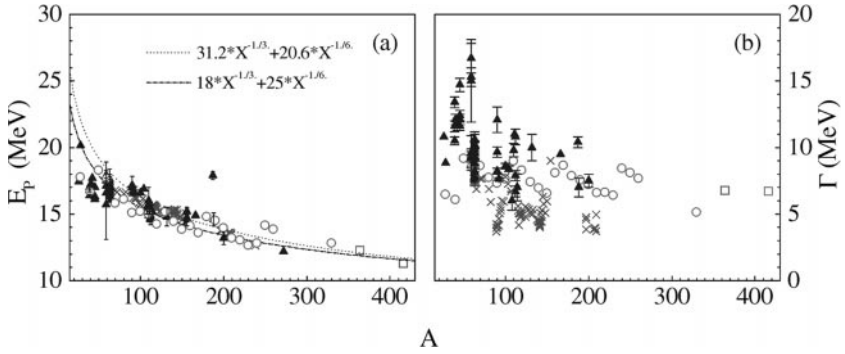

Fig. 1. The calculated results of the peak energy and widths (FWHM) of the GDR against atomic mass number. (a), the crosses and up-triangles represent the experimental peak energy of the GDR. The dotted line and dashed line are the empirical formula for the cold and hot nuclei respectively. The open circles show the calculated results with temperature at 1 MeV and open squares represent the peak energies for SHCS at temperature $T = 2$ MeV. (b) is the same as (a), but the y-axis represents the widths of the GDR

3 Results and discussion

3.1 Systematics of GDR

The calculated results are shown in the Fig. 1a for the peak energy of GDR strength distribution. We select the even-even nuclei across the periodic table. The temperature was set at 1 MeV in the calculations, because many experiments have been done where the nuclear temperature is around 1 MeV. The open circles represent the calculated results. The crosses represent the experimental data of the cold nuclei (photon-nucleus reaction) [19] and the up-triangles are those of the hot nuclei (heavy ion reactions) [1]. The dotted line and the dashed line are given by the empirical formula for the cold and for the hot nuclei respectively. It can be seen, the calculated results agree with the experiment data quite well and also follow the empirical formula. The width of the GDR strength distribution is subtracted by one Lorentz fit. The results are shown in Fig. 1b. It can reproduce the experimental data within the error bar. This indicates that the microscopic Vlasov method is, maybe, reliable to extend to study the spherical super-heavy nuclei and the isospin effects on the GDR in the nuclei not very far from the β stability line.

3.2 Isospin effects on GDR

The isospin effects have been studied in the frame of the microscopic semi-classical Vlasov method. Two points should be emphasized here. One, we have studied the GDR systematically in the Vlasov Frame, then apply it to study the spherical super-heavy nuclei and the isospin effects on the GDR in the nuclei not very far from the β stability line. The experimental results are expected to check whether the model is right in such region. The other, in this theoretical frame, we have considered the neutron and proton potential separately. The different values of the potential parameter U_0 are adopted in order to have the correct number and the same Fermi energy of protons and neutrons in the nucleus. The small isospin effects are observed in the calculations.

Firstly the Ca isotopes have been studied. Figure 2 shows the calculated peak energy and the widths of the GDR strength distribution as the function of (N-Z). The experimental data and our calculations are both lower

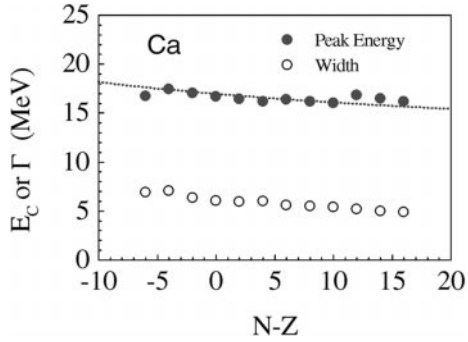

Fig. 2. Calculated results for the Ca isotopes. The solid circles are the peak energy and the open ones are the widths of the GDR. The dotted line is the empirical formula with 1.8 MeV shifted down

than the empirical value for nuclei with atomic mass number A around 40 as shown in Fig. 1a, so the empirical line in Fig. 2 is shifted down 1.8 MeV in order to observe the isospin effects more clearly. The calculated values fit the empirical formula with only A term. It indicates that the dependence shown in the figure may mainly come from the dependence of the mass number A. No obvious dependence on the N-Z is seen. These results are similar to the recent researches via RRPA method for the Ar isotopes [5]. The widths of the GDR strength distribution show the similar behaviors.

In the above study, (Z-N) dependence and A dependence are both included in the Ca or Ar isotopes. Thus, the isospin effects may be covered by mass dependence if it was small. In order to exclude the mass dependence, we have selected three groups of isobars (fixed atomic mass number A) in the light (A=40), intermediate (A=120) and heavy (A=208) mass regions. The results are shown in Fig. 3a–c. We can see small isospin effects on the peak energy of the GDR strength distribution within these three mass regions. The widths also change a little with the isospin (N-Z). It is not difficult to see that the peak energy of the GDR strength distribution increases slightly with the increase of the isospin (N-Z). The peak energy for A=40 isobars increases faster than those of A=120 and A=208 isobars. It can be explained that the isospin effects on the GDR peak energy depend mainly on the (N-Z)/A term. In the experiment, the light isobars are more proper to be selected in the study of the isospin effects on the

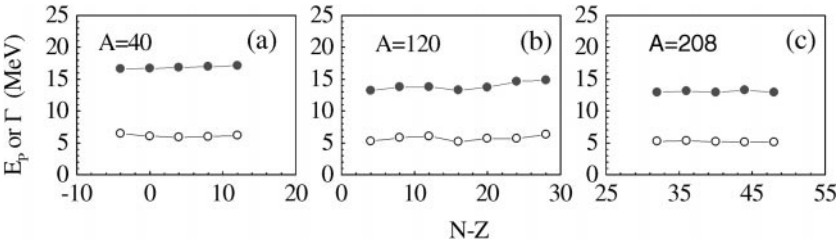

Fig. 3. Calculated results for $A = 40$ (a), 120 (b), 208 (c), respectively. The solid circles are the peak energy and the open ones are the widths of the GDR. The lines guide the eyes

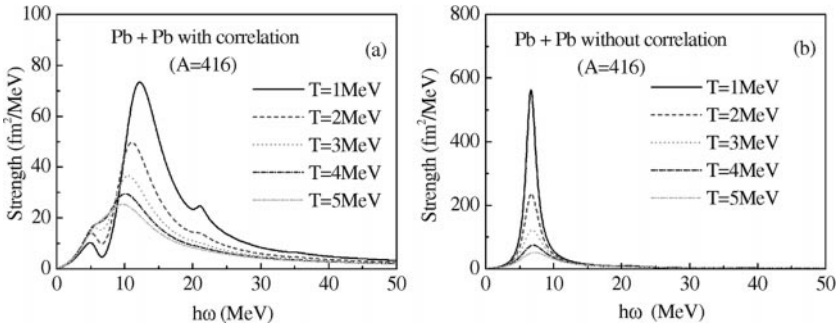

Fig. 4. Temperature dependence of strength distribution of GDR for ^{208}Pb + ^{208}Pb system ($A = 416$): (a) with correlation, (b) without correlation

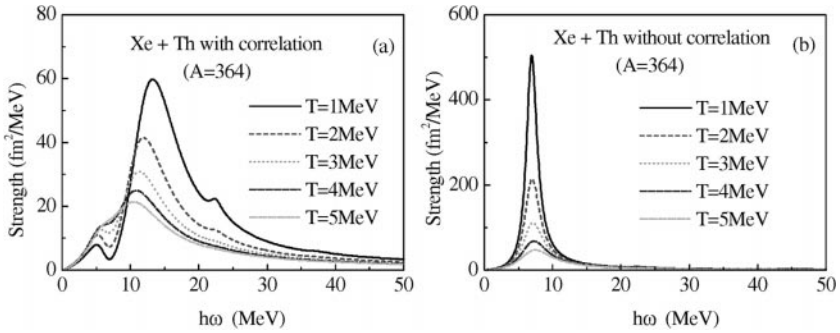

Fig. 5. The same as Fig. 4, but for ^{132}Xe + ^{232}Th system ($A = 364$)

GDR. It is possible now for such experiments because the available Radioactive Ion Beam (RIB) facilities can provide the ions with atomic mass numbers close to 40.

3.3 GDR in SHCS

Study of the SHCS is one of the very interesting subjects for a long time. Recent researches for time scale of the fission process in hot compound nuclei show that the fission delay time is of the order 10^{-20} s [9–10], about ten time longer than the life time of the GDR, which is about 10^{-21} s [20]. So, we may observe the GDR γ rays from the SHCS in very heavy nuclei collisions. Following this idea, two experiments have been done, 12 MeV/u ^{129}Xe on ^{232}Th at Cyclotron of Texas A&M University of United States which is being analyzed by our group and 15 MeV/u ^{208}Pb on ^{208}Pb at RIKEN. In order to understand SHCS possibly formed in these reactions well, we have studied the GDR from the SHCS in the frame of the microscopic semi-classical Vlasov method. The SHCS is generally regarded as largely deformed. However, here we have to suppose that it is spherical because the present model doesn't contain the deformation effects. So we can study the main characteristics of the GDR in SHCS in the present paper.

Figures 4 and 5 show the effects of temperature on the strength distribution of GDR for SHCS formed in ^{208}Pb + ^{208}Pb and ^{132}Xe + ^{232}Th collisions respectively. The corresponding peak energy, widths, fraction of EWSR (Energy Weighted Sum Rule) in the resonance region ($7 \sim 25$ MeV) and the used relaxation time are given in Table 1. The peak energy of GDR strength distribution is also shown in Fig. 1a for the SHCS with A=364 and 416 at $T = 2$ MeV. This temperature is close to the experimental one. The values agree with the empirical formula data. These values need checking with the forthcoming experimental results.

Figures 4a and 5a show the strength distribution of GDR for A=416 and A=364 systems respectively with residual interaction (correlated results) and Figs. 4b and 5b present the calculations without residual interaction (uncorrelated results). In Figs. 4b and 5b, the two-body dissipation (Collision damping) is contained through the relaxation time. If we compare with the final strength distribution calculated with residual interaction (correlated results), we can find that the strength distribution widths of GDR become much larger than in the uncorrelated cases. This is the strength fragmentation effect of the one-

Table 1. the peak energy, widths, fraction of EWSR in the resonance region and the used relaxation time for isovector GDR in ^{132}Xe + ^{232}Th and ^{208}Pb + ^{208}Pb

Nucleus	T (MeV)	Peak Energy (MeV)	Width (MeV)	EWSR (%)	$\hbar/\tau$ (MeV)
^{132}Xe+^{232}Th	1	13.2	7.7	60.6	0.947
	2	11.9	7.6	58.2	1.354
	3	11.3	8.8	55.8	1.856
	4	10.8	10.0	54.0	2.376
	5	10.4	10.5	52.6	2.878
^{208}Pb+^{208}Pb	1	12.2	6.6	62.9	0.899
	2	11.0	7.0	59.6	1.306
	3	10.5	8.3	56.8	1.808
	4	10.1	9.4	54.7	2.328
	5	9.7	9.7	53.1	2.831

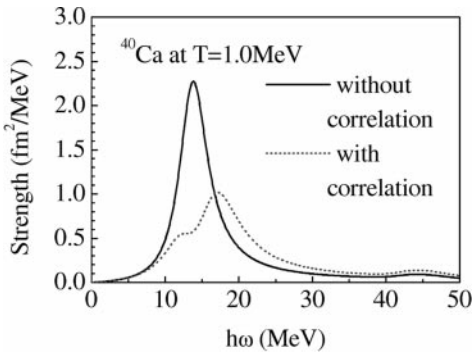

Fig. 6. The comparison of GDR strength distribution in ^{40}Ca with and without correlation at $T = 1.0$ MeV

body theories. This also elucidates a quite complicated interplay between Landau damping (one body damping) and collision damping (two-body damping). In very heavy nuclei, the one-body damping plays an important role in the width spreading of GDR strength distribution compared with two-body damping. It is quite different for the light nuclei, see Fig. 6, the strength distribution width of GDR becomes only a little larger from uncorrelated results to correlated results.

With increasing of the temperature, a clear decrease of the strength allocated in the giant resonance region is observed for both cases of with and without residual interaction as shown in Figs. 4, 5. The fractions of the EWSR decrease from 62.9% to 53.1% for ^{208}Pb + ^{208}Pb and from 60.6% to 52.6% for ^{132}Xe + ^{232}Th, as given in Table 1, with increasing of the temperature. At the same time, the widths become lager and larger. This means that the strength of GDR in SHCS become weaker and weaker and finally quench as the temperature further increases, which is similar to the experimental results for the nuclei around the β stability line. The peak energy is shifted to the low energy side a little with increasing of the temperature in the correlated cases. However, there is no obvious change of peak energies in the uncorrelated cases.

4 Summary

In a summary, within the frame of the microscopic semi-classical Vlasov method with the Wood-Saxon nuclear potential, the calculated results of the systematics of the peak energy and the widths of the GDR strength distribution can reproduce the experimental data and follow the empirical formula in the whole periodic table. The calculations were extended to very heavy nuclei ($A \sim 400$). They need checking with experimental data. The effects of the isospin on the peak energy and widths of the GDR are small. We also observed that these small isospin effects are more obvious in the light nuclei than in the heavy ones. They are proportional to $(N - Z)/A$.

The behaviors of the GDR for the SHCS are also investigated. The main results show that, in the very heavy nuclei, the residual interaction play a fundamental role in the widths of GDR strength distribution, i.e. the collision damping predominates the damping of the GDR comparing with the Landau damping. The temperature plays another important role in describing the GDR for SHCS. There is a noticeable quenching of the response strength at high temperature and the widths obviously increase with the temperature. A slow decreasing of the peak energy of GDR for the SHCS with temperature increasing is also obtained.

Finally, we have found some interesting behaviors about the GDR in spherical SHCS and the isospin effects on the GDR in the isobars although the present microscopic semi-classical Vlasov methods has some limitations. In the present model, the studied nuclei are not very far from the β stability line, assuming that the nuclei are spherical and the residual interaction parameters are somewhat uncertain. An improved Vlasov model, which contains the deformation and the parameters suitable to the nuclei very far from the β stability line, is under consideration.

The authors thank Professor J. B. Natowitz and Dr. R. Wada from the Cyclotron Institute of the Texas A&M University for their fruitful discussions and all helps. This work is supported by the National Science Foundation of China under Grant No. 19675059, 19675060, 19705012, 19725521 and Shanghai Science and Technique Development Foundation under Grant No. 96XD14011, 97QA14038 and 97XD14020.

References

1. J.J. Gaard et al., Ann. Rev. Nucl. Part. Sci. **42** (1992) 483
2. K.A. Snover et al., Ann. Rev. Nucl. Part. Sci. **36** (1986) 545
3. V. Baran et al., Nucl. Phys. A**599** (1996) 29c
4. Z.Y. Ma et al., Nucl. Phys. A**627** (1997) 1
5. Z.Y. Ma et al., Prog. Theor. Phys. **98** (1997) 917
6. N.V. Giai et al., Phys. Rev. C**57** (1998) 1204
7. I. Hamamoto, H. Sagawam, X.Z. Zhang, Nucl. Phys. A**626** (1997) 669

8. I. Hamamoto et al., Phys. Rev. C**57** (1998) R1064
9. W.Q. Shen et al., Phys. Rev. C**36** (1987)
10. M. Thoennessen et al., Phys. Rev. Lett., **71** (1993) 4303 and references therein
11. J.S. Wang et al., Progress in Research (CYCLOTRON INSTITUTE, TAMU, USA), (1997–1998) II33-34
12. R. Wada et al., Progress in Research (CYCLOTRON INSTITUTE, TAMU, USA), (1997–1998) II35-38
13. D.M. Brink et al., Nucl. Phys. A**456** (1986) 205
14. G.F. Burgio et al., Nucl. Phys. A**476** (1988) 189
15. Y.H. Cai et al., Phys. Rev. C**39** (1989) 105
16. G.F. Burgio, A. Bonasera and M. Di Toro (Private communication)
17. H.S. Köhler, Nucl. Phys. A**438** (1985) 564; H.S. Köhler and D.S. Nilsson, Nucl. Phys. A**417** (1984) 541
18. B.S. Zhou et al., Z. Phys. A**352** (1995) 119
19. S.S. Dietrich et al., Atomic Data and Nucl Data Tables, **38** (1988) 199
20. J. Kasagi and K.Yoshida, Nucl. Phys. A**569** (1994) 195c; K. Yoshida et al., Phys. Lett. B**245** (1990) 7